

## Biocomposites based on selenium-substituted hydroxyapatite

*O.A. Golovanova\**, *A.I. Karpova*

*Omsk State University F.M. Dostoevsky, Omsk, Russia*  
*golovanoa2000@mail.ru*

**Abstract.** When creating biocompatible calcium phosphate materials with good bioresorbability, calcium hydroxyapatite (HA) is used, which has a similar structure to bone mineral and has good biocompatibility, bioactivity and high resistance to proteins, chemotherapeutic drugs and antigens. The synthesis of HA/SeO<sub>3</sub> was carried out and it was shown that selenite ions can be included in the structure of HA, which is the predominant phase, the crystallites have a lamellar morphology and the same size, which indicates that the replacement of HA with SeO<sub>3</sub><sup>2-</sup> ions does not lead to a change in its structure. The solubility of the modified samples in 0.9% NaCl and acetate buffer increases compared to pure HA, which confirms the inclusion of selenite ions in the HA structure. The synthesis of HA/SeO<sub>3</sub>/chitosan composites was carried out and it was found that the predominant phase is HA, and the morphology of SeO<sub>3</sub>-HA/chitosan aggregates are complex bulk particles of irregular shape. Dissolution of samples in 0.9% NaCl/acetate buffer of the HA/SeO<sub>3</sub> composition occurs less intensively than for samples of the HA/SeO<sub>3</sub>/chitosan composition, which allows the former to be used in the case of passive resorption, and HA/SeO<sub>3</sub>/chitosan composites for active resorption.

**Keywords:** hydroxyapatite, chitosan, selenium, composite, morphology

### 1. Introduction

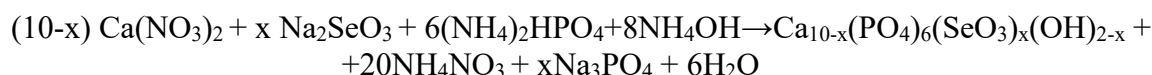
Nowadays, of particular interest in medicine is the possibility of reconstructing bone tissue using non-toxic materials, which over time are resorbed in the body and replaced by new bone tissue. Such materials consist of an inorganic and an organic phase. Calcium phosphates (CP) are widely used as inorganic materials, since they consist of Ca<sup>2+</sup> and PO<sub>4</sub><sup>3-</sup> ions necessary for the construction of bone tissue [1–4]. To create biocompatible calcium phosphate materials with good bioresorbability, calcium hydroxyapatite (HA) is used, which has a similar structure to bone mineral and has good biocompatibility, bioactivity and high resistance to proteins, chemotherapeutic drugs and antigens [5–8]. Research has shown that hydroxyapatite modified by ion doping also has some special biological properties.

The element selenium has antitumor, antibacterial and anti-aging effects, and can also enhance human immunity. Selenium intake plays an important role in bone formation [3, 8]. Therefore, it is very important to obtain a multifunctional new bone repair material with good osteoconductivity, as well as antitumor, antibacterial and other effects by incorporating selenium into hydroxyapatite [9].

Selenium-enriched HA is most often prepared by wet deposition methods using SeO<sub>3</sub><sup>2-</sup> ions as a source of selenium. The use of natural resources such as cuttlefish bone to produce composites is a promising direction because they contain, in addition to calcium, many useful ions found in human bones [10, 11]. The purpose of the work is to synthesize and study the physicochemical properties of HA/SeO<sub>3</sub>/chitosan composites.

### 2. Materials and methods

The synthesis of composites is carried out by the “wet method” at room temperature. The synthesis is based on the reaction:



The synthesis is carried out at a constant concentration of Ca<sup>2+</sup> (0.068 mol/L). The concentrations of HPO<sub>4</sub><sup>2-</sup> and SeO<sub>3</sub><sup>2-</sup> ions vary so that  $n1 = \text{SeO}_3^{2-} / (\text{HPO}_4^{2-} + \text{SeO}_3^{2-})$  varies from

1.5; 3.0; 5.0; 7.5; 10 g/L, and  $n_2 = \text{Ca}^{2+} / (\text{HPO}_4^{2-} + \text{SeO}_3^{2-}) = 1.67$ . Add 25% aqueous  $\text{NH}_4\text{OH}$  solution to pH 10.5. The precipitate is filtered 2 days after the solution is completely added.

Next, the precipitate is dried in an oven at a temperature of  $T = 80^\circ\text{C}$  to completely remove unbound water. The dried sediment is transferred to a container and weighed on an analytical balance.

To obtain chitosan gel, we used low molecular weight chitosan obtained from the shells of Kamchatka crabs without any impurities. A 2% solution of chitosan was prepared in 0.5% acetic acid for 24 hours. The pH of the resulting gel was kept at least 7.0. The resulting gel forms a thin, moderately soluble film on the skin or polymer substrate within 10 minutes. Powdered material (HA/ $\text{SeO}_3$  (3.0, 7.5, 10 g/L)) was introduced into the resulting gel in an amount of 10, 30 wt.% and subjected to intensive stirring. The resulting foam was placed in a crucible and dried at  $T = 22\text{--}25$  and  $200^\circ\text{C}$ .

Determination of the concentration of calcium ions during the study of the solubility of synthetic calcium phosphates is carried out by direct potentiometry using an ion-selective electrode.

Orthophosphate ions in the presence of excess molybdate in an acidic environment form phosphomolybdic heteropolyacid (PMH). Using a KFK-2 device, using a red light filter ( $\lambda = 690$  nm) and cuvettes with a layer thickness of 2 cm. The determination is repeated three times and a calibration graph is constructed using the average optical densities:  $D = f\{C(\text{PO}_4^{3-})\}$ , the regression equation is calculated.

Selenite ions were determined by the photometric method. The method is based on the catalytic action of Se(IV) in the reaction of methylene blue with sulfide ions. Spectrophotometer B-1100,  $\lambda = 618$ . The error of determination is within 2–4%.

The phase composition of the obtained samples was studied using X-ray diffraction. (D8 Advance diffractometer, Bruker Company). In order to obtain additional information about the composition of the synthesized samples, the method of infrared spectroscopy was used. IR spectra were obtained on an FSM 2202 spectrophotometer, Infracap, Russia. The detection limit was 5%.

The sediments obtained during the syntheses are examined by optical microscopy using a binocular microscope of the XSP-104 series.

To study the stability of calcium phosphate samples synthesized under various conditions, they are dissolved in a solution of NaCl 0.9%, and acetate buffer.

### 3. Results and its discussion

The study of solid phases by X-ray phase analysis showed that the main mineral component is hydroxyapatite. The main intense lines of hydroxyapatite according to the 2 $\theta$  school are angles 23.0; 25.9; 31.9; 39.8; 49.5 and 53.3 (Fig. 1). Also, in the diffraction patterns at a concentration of selenite ions of 7.5 g/L, angles of 12.14; 17.82; 31.75, which characterizes the presence  $\text{CaSeO}_3 \cdot \text{H}_2\text{O}$ . Using the Debye-Scherrery formula, the average crystallite sizes were calculated from the diffraction patterns of the samples HA/ $\text{SeO}_3$ . It is clear from the data that the crystallites have the same size, this indicates that the replacement of HA with  $\text{SeO}_3^{2-}$  ions does not lead to distortion of its structure (1.5 g/L – 0.53 Å; 3.0 g/L – 0.54 Å; 5.0 g/L – 0.54 Å; 10.0 g/L – 0.55 Å).

Using Fourier transform infrared spectroscopy, it was found that the synthesized  $\text{SeO}_3^{2-}$ /HA samples have the entire set of bands characteristic of calcium phosphates and selenium ions. In the composition of  $\text{SeO}_3^{2-}$ /HA, the IR spectra show absorption bands of the O-P-O bond in  $\text{PO}_4^{3-}$  and  $\text{HPO}_4^{2-}$ , where the absorption maxima are 1000, 1034  $\text{cm}^{-1}$  – stretching vibrations, 563  $\text{cm}^{-1}$ , 604  $\text{cm}^{-1}$  – bending vibrations (Fig. 2).

Vibrations of the C-O bond in  $\text{CO}_3^{2-}$  are observed at 872–874  $\text{cm}^{-1}$  (carbonate-substituted hydroxyapatite is B-type). Vibrations characteristic of the Se-O bond are observed in the region of 820–890  $\text{cm}^{-1}$ . The intensity of the absorption bands increased with increasing  $\text{SeO}_3^{2-}$  concentration;

these bands are related to symmetric and asymmetric vibrations of the Se-O bond. This is proven by the inclusion of selenium ions in the HA structure.

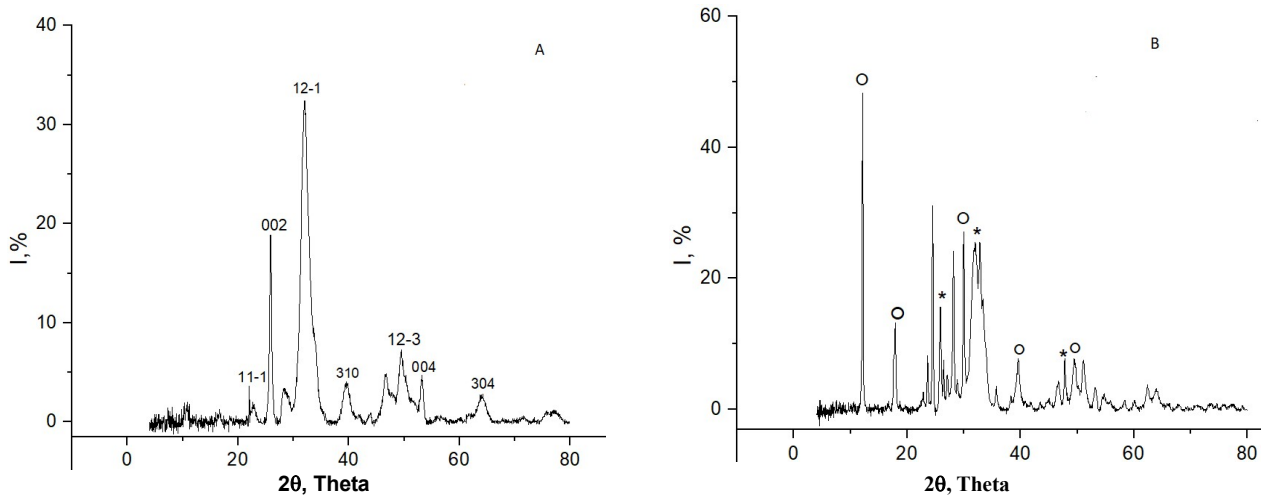


Fig. 1. X-ray diffraction patterns of HA/SeO<sub>3</sub> samples with different concentrations of selenite ions (A – 1.5; B – 7.5 g/l, \*HA, ° – CaSeO<sub>3</sub>\*H<sub>2</sub>O).

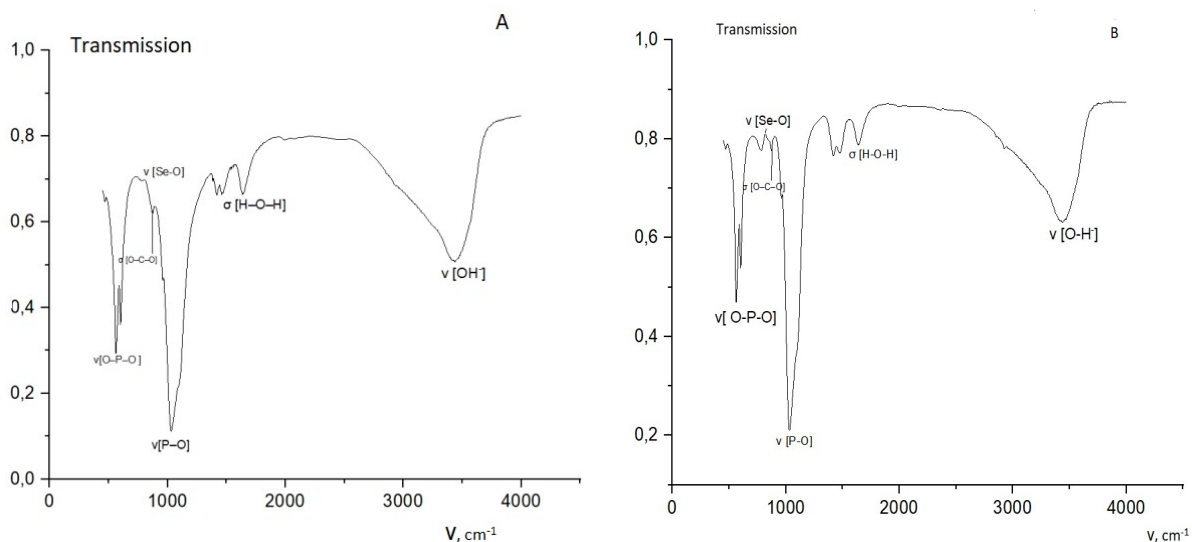


Fig. 2. IR spectra of synthesized HA-SeO<sub>3</sub>, with different concentrations of SeO<sub>3</sub><sup>2-</sup> ions, g/l (A – 1.5; B – 7.5).

Chemical analysis of the supernatant showed the presence of selenium ions in the resulting solid phases. The Ca/P coefficient was calculated, which for biogenic hydroxyapatite is 1.67. With an increase in the concentration of selenite ions in the solution during synthesis, the Ca/P coefficient increases and amounts to 2.07, which confirms the possibility of including the selenite ion in the HA structure at the position of phosphate ions.

The study of solid phases by X-ray phase analysis in the system Ca(NO<sub>3</sub>)<sub>2</sub>-Na<sub>2</sub>SeO<sub>3</sub>-(NH<sub>4</sub>)<sub>2</sub>HPO<sub>4</sub>-NH<sub>4</sub>OH-H<sub>2</sub>O – chitosan showed that the main mineral component is hydroxyapatite.

Using Fourier transform infrared spectroscopy, it was found that the synthesized SeO<sub>3</sub><sup>2-</sup> HA/chitosan samples have the entire set of bands characteristic of calcium phosphates and selenium ions. In the composition of SeO<sub>3</sub><sup>2-</sup>/HA/chitosan, absorption bands of the O-P-O bond in PO<sub>4</sub><sup>3-</sup> and HPO<sub>4</sub><sup>2-</sup> appear in the IR spectra, where the absorption maxima are 1000, 1034 cm<sup>-1</sup> – stretching vibrations, 563 cm<sup>-1</sup>, 604 cm<sup>-1</sup> – bending vibrations (Fig. 3). Vibrations of the C-O bond in CO<sub>3</sub><sup>2-</sup> are observed at 872–874 cm<sup>-1</sup> (carbonate-substituted hydroxylapatite is B-type).

Vibrations characteristic of the Se-O bond are observed in the region of 820–890  $\text{cm}^{-1}$ . The intensity of the absorption bands increased with increasing  $\text{SeO}_3^{2-}$  concentration; these bands are related to symmetric and asymmetric vibrations of the Se-O bond. A wide absorption band in the far region of the spectrum at 3237, 2955  $\text{cm}^{-1}$  relates to stretching and bending vibrations of –OH and –NH<sub>2</sub> groups. These groups are involved in the formation of intra- and intermolecular bonds in the chitosan molecule. For chitosan in the composition of the composite, absorption bands are visible with a frequency of 3737  $\text{cm}^{-1}$ , related to vibrations of the O-H bond, and at a frequency of 1436  $\text{cm}^{-1}$ , the bending vibration of the amino group –NH<sub>2</sub>.

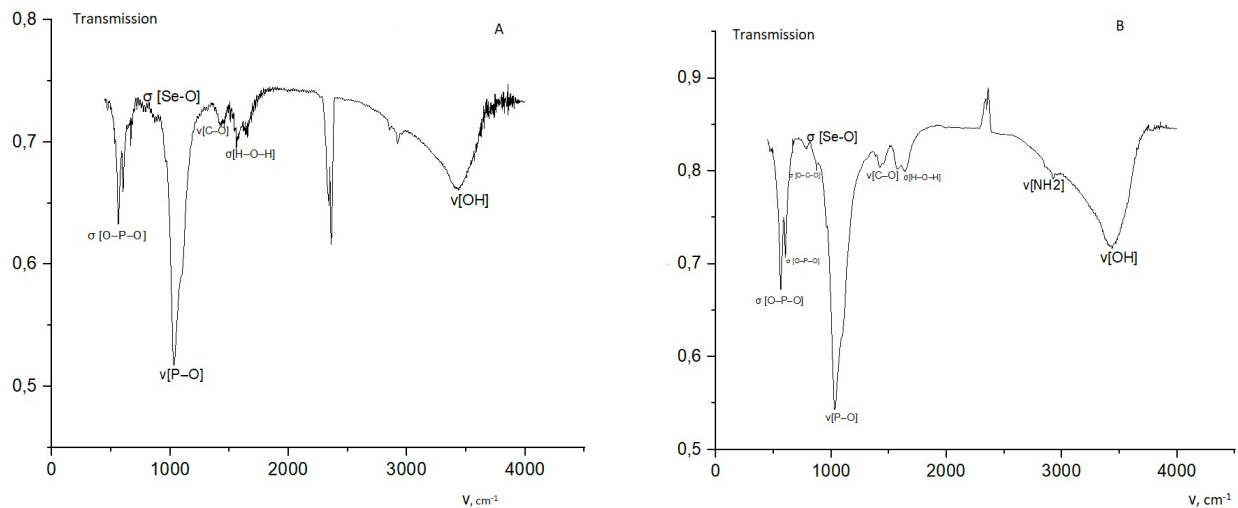


Fig. 3. IR spectra of HA/SeO<sub>3</sub>/chitosan samples: A) HA/SeO<sub>3</sub>(3.0 g/L)/chitosan, 10%; B) HA/SeO<sub>3</sub>(3.0 g/L)/chitosan, 30%.

The morphology of solid phase particles was determined using optical microscopy. From Figure 4 shows that the surface of SeO<sub>3</sub>-HA powder particles has a lamellar morphology, typical of calcium orthophosphate and often observed in biogenic and natural apatites. The addition of chitosan leads to a change in the morphology of the particles, forming complex voluminous particles of irregular shape.

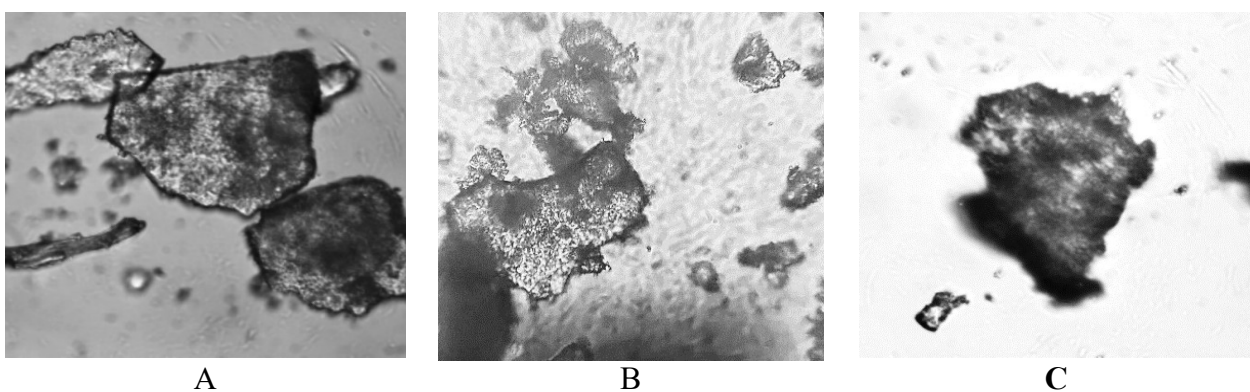


Fig. 4. Type of particles of SeO<sub>3</sub>/HA composites with different contents of selenite ions, g/L: A – 7.5; B – SeO<sub>3</sub>/HA/chitosan, 30%; C – HA/SeO<sub>3</sub> (10.0 g/L)/chitosan, 10%, (magnification 10x40).

The dissolution patterns of HA-SeO<sub>3</sub> composites were carried out for 2 hours in 0.9% NaCl to study the biodegradability of the samples. The solubility of samples containing from 1.5 to 3.0 g/L increases compared to pure HA, which indicates the inclusion of selenite ions in the HA structure. At high  $\text{SeO}_3^{2-}$  concentrations, the solubility of the samples decreases, since selenite ions are

adsorbed on the surface of the sample and the insoluble compound  $\text{CaSeO}_3$  is formed (Solubility product =  $4.7 \cdot 10^{-6}$ ), Table 1.

The patterns of dissolution of HA- $\text{SeO}_3$  composites in acetate buffer (pH = 5.5) showed that the initial dissolution rate for samples increases with rising content of selenite ions in samples with a concentration of 1.5; 3.0; 5.0 g/L, which confirms the likelihood of selenite ions entering the HA structure. In samples containing selenite ions of 7.5 and 10.0 g/L, the dissolution rate decreases due to the adsorption of selenite ions on the surface of the samples.

**Table 1.** Initial dissolution rates.

C selenite ions in solution, g/ L	Speed, $\text{min}^{-1}$ , in 0.9% NaCl	Speed, $\text{min}^{-1}$ , in acetate buffer
0	0.011	0.011
1.5	0.015	0.040
3.0	0.014	0.061
5.0	0.003	0.079
7.5	0.004	0.020
10.0	0.013	0.043

The dissolution patterns of HA- $\text{SeO}_3$ /chitosan composites were carried out in 0.9% NaCl to study the biodegradability of the samples. It has been established that with an increase in the content of selenite ions, the concentration of calcium ions in the solution increases. Based on the obtained experimental dependences  $p\text{Ca} = f(t)$ , the initial values of the rates of release of calcium ions in solution were calculated (Table 2).

**Table 2.** Value of initial dissolution rates.

HA/ $\text{SeO}_3$ / chitosan		Speed, $\text{min}^{-1}$ , in 0.9% NaCl	Speed, $\text{min}^{-1}$ , in acetate buffer
C selenite ions in solution, g/L	Solid phase content, %		
3.0	10	0.006	0.042
7.5		0.033	0.017
10.0		0.050	0.012
3.0	30	0.001	0.049
7.5		0.025	0.009
10.0		0.048	0.015

From the data obtained it is clear that the initial dissolution rate for the samples increases with increasing content of selenite ions in the samples. The increase in speed is associated with greater solubility of calcium selenite (Solubility product =  $4.7 \cdot 10^{-6}$ ). For samples containing 30% solid phase, the same dependences are observed as for samples with 10% solid phase. The patterns of dissolution of HA- $\text{SeO}_3$  composites were carried out in acetate buffer (pH = 5.5). It was found that the dissolution rate for samples decreases with increasing content of selenite ions in the samples, which is associated with the formation of chitosanium ion  $\text{C}_6\text{H}_9\text{NH}_3^+$ , which binds to  $\text{PO}_4^{3-}$  ions and imparts viscosity of the solution.

#### 4. Conclusion

The synthesis of HA/ $\text{SeO}_3$  was carried out: the study of the solid phase by X-ray diffraction and IR spectroscopy showed that selenite ions can be included in the structure of HA, which is the predominant phase; particles have a lamellar morphology, and the same size, this indicates that the replacement of HA with  $\text{SeO}_3^{2-}$  ions does not lead to a change in its structure; the solubility of the modified samples in 0.9% NaCl and acetate buffer increases compared to pure HA, which confirms the inclusion of selenite ions in the HA structure.

The synthesis of HA/SeO<sub>3</sub>/chitosan composites was carried out: the study of the composites by X-ray diffraction and IR spectroscopy showed that the predominant phase is HA.

When comparing the synthesized samples: the crystallite sizes in the HA/SeO<sub>3</sub> samples are close to those in the HA/SeO<sub>3</sub>/chitosan composites; the addition of chitosan leads to a change in the morphology of the particles, forming complex bulk particles of irregular shape; dissolution of samples in 0.9% NaCl/acetate buffer of the HA/SeO<sub>3</sub> composition occurs less intensively than for samples of the HA/SeO<sub>3</sub>/chitosan composition, which allows the former to be used in the case of passive resorption, and HA/SeO<sub>3</sub>/chitosan composites for active resorption.

### Acknowledgement

The work was carried out within the framework of the state assignment of the Ministry of Science and Higher Education of the Russian Federation (topic No. 075-03-2023).

### 5. References

- [1] E. Amenta, H.E. King, H. Petermann, et al., Vibrational spectroscopic analysis of hydroxyapatite in HYP mice and individuals with XLH, *Therapeutic Advances in Chronic Disease*, **9**(12), 268, 2018, doi: 10.1177/2040622318804753
- [2] V.M. Wu, M.K. Ahmed, M.S. Mostafa, et al., Empirical and theoretical insights into the structural effects of selenite doping in hydroxyapatite and the ensuing inhibition of osteoclasts, *Materials Science & Engineering C*, vol. **117**, 111257, 2020, doi.org/10.1016/j.msec.2020.111257
- [3] I. Mocenic, J. Kolic, R. Nisevic, et al., Prenatal selenium status, neonatal cerebellum measures and child neurodevelopment at the age of 18 months, *Environ. Res.*, **176**, 108529, 2019, doi: 10.1016/j.envres.2019.108529
- [4] J.-Z. Chu, X.-Q. Yao, C. Si, et al., Responses of physiological traits and nutritional ingredients content in flowers of medicinal chrysanthemum to Selenium Application at Different Growth Stages, *Journal of Food and Nutrition Research*, vol. **2**(9), 575, 2014, doi: 10.12691/jfnr-2-9-8
- [5] V. Dokic, A. Glushkova, P. Andricevic, et al. Photovoltaic perovskites for high sensitive X-ray detection, *Materials Research Society of Serbia, Belgrade*, 50, 2019.
- [6] V. Uskokovic, M.A. Iyer, V.M. Wu, One ion to rule them all: combined antibacterial, osteoinductive and anticancer properties of selenite-incorporated hydroxyapatite, *J. Mater. Chem. B*, **5**, 1430, 2017, doi: 10.1039/C6TB03387C
- [7] J.J. Cao, B.R. Gregoire, H. Zeng, Selenium deficiency decreases antioxidative capacity and is detrimental to bone microarchitecture in mice, *J. Nutr.*, vol. **142**, 1526, 2012, doi: 10.3945/jn.111.157040
- [8] K.K. Vekariya, J. Kaur, L. Tikoo, Alleviating anastrozole induced bone toxicity by selenium nanoparticles in SD rats, *Toxicol. Appl. Pharmacol.*, vol. **268**, 212, 2013, doi: 10.1016/j.taap.2013.01.028
- [9] B. Alkan, S. Durukan Complete chemical and structural characterization of hydroxyapatite containing selenium, *J. Mater. Sci.: Mater. Med.*, **33**, 5, 2022, doi: 10.1007/s10856-021-06631-6
- [10] D. Depan, T.C. Pesacreta, R.D.K. Misra, The synergistic effect of a hybrid graphene oxide–chitosan system and biomimetic mineralization on osteoblast functions, *Biomater. Sci.*, **2**(2), 264, 2014, doi: 10.1039/C3BM60192G
- [11] D. Depan, P.K. Venkata, B. Girase, et al., Organic/inorganic hybrid network structure nanocomposite scaffolds based on grafted chitosan for tissue engineering, *Acta Biomater.*, vol. **7**(5), 2163, 2011, doi: 10.1016/j.actbio.2011.01